

Journal of Materials Chemistry C

Accepted Manuscript



This is an *Accepted Manuscript*, which has been through the Royal Society of Chemistry peer review process and has been accepted for publication.

Accepted Manuscripts are published online shortly after acceptance, before technical editing, formatting and proof reading. Using this free service, authors can make their results available to the community, in citable form, before we publish the edited article. We will replace this *Accepted Manuscript* with the edited and formatted *Advance Article* as soon as it is available.

You can find more information about *Accepted Manuscripts* in the [Information for Authors](#).

Please note that technical editing may introduce minor changes to the text and/or graphics, which may alter content. The journal's standard [Terms & Conditions](#) and the [Ethical guidelines](#) still apply. In no event shall the Royal Society of Chemistry be held responsible for any errors or omissions in this *Accepted Manuscript* or any consequences arising from the use of any information it contains.

**Synthesis of Monodispersed Polystyrene-Silver Core-Shell Particles and Their
Application for Fabrication of Stretchable Large-Scale Anisotropic
Conductive Films**

Hsueh-Yung Chen,^a Hsiu-Ping Shen,^b Hung-Chin Wu,^a Man-Sheng Wang,^c Chia-Fen
Lee,^d Wen-Yen Chiu,^{*abc} Wen-Chang Chen,^{*a}

*To whom all correspondence should be addressed.

Wen-Yen Chiu (e-mail: ycchiu@ntu.edu.tw) ; Wen-Chang Chen

(e-mail: chenwc@ntu.edu.tw)

Abstract

Monodispersed core-shell conductive particles are designed and produced as efficient electron transporting materials for anisotropic conductive films. Traditionally, particle size control was required usually owing to the demand of anisotropic conductive films. Here, an innovative and facile method is proposed to prepare the large-scale anisotropic conductive films incorporating with the organic/inorganic core-shell conductive particles. First of all, monodispersed polystyrene-silver (PS-Ag) core-shell particles were prepared by emulsifier-free emulsion polymerization and modified electroless plating process. A series of variables was used to synthesize the PS-Ag conductive particles to enhance the mobility of electrons in a media. The resulting PS-Ag conductive particles had excellent bulk conductivity with Ag nanoshells compactly embedded on the surface of PS colloids. In addition, the PS-Ag conductive particles were further mixed with soft latex particles of poly(styrene-co-butyl acrylate), P(St-BA), and then followed by the film-forming process. After the formation of large-scale anisotropic conductive films by gravity sedimentation method, a remarkable flexible behavior with good conductivity was obtained. The presented method shows the significance of developments in electronic fields and is expected to be a practical, facile, and general approach for the fabrication of the anisotropic conductive films with good flexibility and stretchability.

Keywords: polystyrene-silver core-shell particles, soft latex, poly(styrene-co-butyl acrylate) particles, gravity sedimentation, anisotropic conductive film.

Introduction

As shown in recent studies, the fabrication of organic–inorganic composite particles featuring specifically metallic shell around dielectric core has received considerable attention because of the extensive applications in electronics, surface-enhanced Raman scattering (SERS), sensor, catalysis, photonic crystal, biochemistry, and so on.¹⁻¹⁰ For example, with the merits of high conductivity and uniform diameter, the organic–inorganic composite particles have been widely used for adding into the insulating polymeric matrices to form the anisotropic conductive films (ACFs). Traditional anisotropic conductive films are manufactured via using the metallic particles or organic–inorganic composite particles as fillers in an adhesive polymeric matrix and forming them into solid films.¹¹⁻¹² Organic–inorganic composite particles with a few microns of diameter are usually coated by highly conductive metals such as gold or silver. Meanwhile, the elastic cores have similar coefficient of thermal expansion compared to the adhesive polymeric matrices and provide a large contact area between the interconnection of two electrodes after thermocompression. In particular, using silver as the shell materials for organic–inorganic composite particles has become an extremely important issue due to its eminent combination of properties and potential applications.

Up to now, a variety of synthetic strategies has been reported and used to deposit the metal onto the surface of dielectric cores with the desired functionality and chemical composition, such as sonochemical deposition,¹³⁻¹⁴ pulsed laser irradiation,¹⁵ ultrasound irradiation,¹⁶ in-situ reduction,¹⁷⁻²⁰ electrodeposition,²¹ layer-by-layer self-assembly,²²⁻²⁶ and electroless plating.²⁷⁻³³ Among the above-mentioned researches, electroless plating process is regarded as the promising candidate for the preparation

of organic–inorganic composite particles with continuous and uniform shells owing to the facile, convenient, simple process. However, the conventional electroless plating process still has some problems to be solved, for instance, the complicated pretreatment (roughening, sensitization, and activation) during the reduction of metal ions, difficult coating a metal layer onto the surface of polymer colloids in virtue of the presence of hoop stresses and the peel-offed situation of the metallic shells from the polymeric spheres.

Attributed to the rapidly raising requirement for humanity in the electronic products, the development of devices became very important in the field of future electronics. So far, there are conspicuous growth in the electronic products, even wearable and foldable electronic products, such as flexible displays, medical devices, smart skins, soft energy devices, and so on.³⁴⁻⁴² Although the anisotropic conductive films could be applied to devices,⁴³⁻⁴⁷ the mentioned problems still restricted the progress in the electronic field. For the sake of settling the referred problems, here we proposed a facile synthetic route to prepare monodispersed polystyrene-silver core-shell particles with high conductivity via the combination of modified electroless plating and in-situ reduction. At first, monodispersed polystyrene particles with the functional groups of mercaptan (-SH) were successfully synthesized by emulsifier-free emulsion polymerization. Then, instead of using the conventional electroless plating process like prior literatures, a modified electroless plating method without the step of roughing was used to acquire a dense shell on the surface of the polystyrene particles. In our previous work, the introduction of soft matrix into the conductive films had proved to enhance the flexibility substantially.⁴⁸⁻⁴⁹ Herein, the same method of forming the conductive films was extended and further applied to fabricate a novel large-scale anisotropic conductive film with good flexibility and

stretchability via gravity sedimentation method. In order to differentiate it from the commercial products of anisotropic conductive film, the samples were named as “L-anisotropic conductive film”. In this work, L-anisotropic conductive films could be fabricated easily via gravity sedimentation method and utilized in various fields from different manufacture ways. Moreover, the stretchable L-anisotropic conductive films could be integrated facilely and possessed stable characteristics under strain. The method is expected to have great potential for the preparation of anisotropic conductive films and wide applications in the forward-looking electronics.

Experiments

Materials

Monomers, n-butyl acrylate (BA) and styrene (St), and triethoxyvinylsilane (TEVS), (3-Mercaptopropyl)trimethoxysilane (MPTS), sodium dodecyl sulfate (SDS), tin(II) chloride, ammonia solution (35 wt.%), Sodium hydroxide (NaOH), and D(+)-glucose were purchased from Acros. Silver nitrite was obtained from Showa. Divinylbenzene (DVB), Sodium citrate tribasic dihydrate, 2,2'-azobisisobutyronitrile (AIBN), and hydrochloric acid (37 wt.%) were purchased from Sigma-Aldrich. Potassium persulfate (KPS) was obtained from Alfa. Methanol (analytical grade) was purchased from ECHO Chemical. N-butyl acrylate (BA), styrene (St) and divinylbenzene (DVB) were purified by distillation under the reduced pressure and stored at 4°C before the use. All other reagents were used as received. Only deionized water could be used throughout the study.

Synthesis of PS latex with functional groups of mercaptan via emulsifier-free emulsion polymerization

At first, 10 g of styrene monomer was added into 180 g of deionized water. All reagents were introduced into a four-necked glass cylindrical reactor equipped with a water condenser, a mechanical stirrer, and then purged with nitrogen gas. The above-mentioned mixture was pre-heated at 75 °C for 30 minutes, followed by adding an initiator solution of 0.5 g of KPS dissolved in 10 g of deionized water. The reaction was kept at 75 °C and 200 rpm of stirring speed for 4 hours. In the end of emulsifier-free emulsion polymerization, polystyrene (PS) latex with 60-70 % of conversion was obtained. After that, the PS latex was swollen by the different weight ratios of DVB, St and TEVS for 24 hours at room temperature in the second stage. Then, the latex solution was pre-heated to 75 °C for 30 minutes, followed by the addition of 10 g of initiator solution containing 0.5 g of KPS to start the reaction in a nitrogen atmosphere. Emulsifier-free emulsion polymerization was allowed to proceed with 200 rpm of stirring speed at 75 °C for 24 hours, and the PS latex with SiOH groups was obtained. The equivalent molar content of MPTS compared with the amounts of TEVS in the above-mentioned solution was dropped into the produced latex and reacted at room temperature for 3 hours. Finally, monodispersed spheres with the functional groups of mercaptan (PS-SH) were obtained after centrifugation for three times and dispersed in 120 g of deionized water. The samples were coded as PS_{4/3.5/2.5}, PS_{4/2/6}, and PS_{4/2/10}, where the numbers meant the different weight ratios of DVB, St and TEVS swollen in the second stage.

***In-situ* reduction of Ag nanoparticles on PS particles with functional groups of mercaptan by modified electroless plating process**

In a typical experiment, the sensitization solution was prepared by dissolving 0.2

g of SnCl_2 and 0.074 g of HCl in 10 g of deionized water. The PS particles were sensitized under magnetic stirring in a water bath at room temperature. After 1 hour, the mixture was centrifuged three times to remove the excess Sn^{2+} ions and re-dispersed in deionized water. The silver ammonia solution ($\text{Ag}(\text{NH}_3)_2^+$) was prepared from AgNO_3 solution. 30 g of 4 wt.% NaOH was dropped into 24 g of 12.5 wt.% AgNO_3 solution and formed the brown precipitation, followed by adding 6 g of 28 wt.% NH_3 solution slowly to dissolve the precipitation. After the disappearance of precipitate, 2.6 g of sodium citrate tribasic dehydrate was added into the mixture. Then the prepared silver ammonia solution was dropped into 30 g of 10 wt.% Sn-functionalized PS latex with magnetic stirring for 3 hours at room temperature. Then, 2 wt.% glucose solution was utilized to reduce the Ag ions. PS-Ag core-shell particles were obtained after three times of centrifugation and dispersed in 120 g of deionized water. The designed samples were coded per the following rules, for example, $\text{PS}_{4/2/6}\text{-Sn-SC-Ag}_{80}$ where Sn symbolized the addition of SnCl_2 for sensitization, SC represented the postponed addition of sodium citrate tribasic dehydrate which was dropped into the mixture 2 hours later, and the number 80 was the weight percentage of the silver content in the core-shell particle.

Synthesis of P(St-BA) latex

The P(St-BA) latex was synthesized via emulsion polymerization by using sodium dodecyl sulfate (SDS) as the surfactant. At the beginning, 1 g of surfactant SDS was dissolved in 100 g of deionized water in a three-necked flask and stirred with a magnetic stirrer. The pH value was adjusted to 7.0. Mixed monomers (2.8 g of styrene and 8.4 g of n-butyl acrylate) with the initiator 2,2'-azobisisobutyronitrile (AIBN) were added into the solution. The oil/water emulsion was stirred magnetically for 1 hour, followed by sonication (frequency cycle = 1, amplitude = 100 %) for 30

minutes in a water bath. After sonication, the emulsion was then undergoing polymerization at 90 °C for 2 hours with magnetically stirring under a nitrogen atmosphere. Finally, the P(St-BA) latex with a St/BA weight ratio of 1/3 was prepared.

Preparation of PS-Ag /P(St-BA) large-scale anisotropic conductive films

The PS-Ag core-shell particles were mixed with the different amounts of P(St-BA) latex. After mixing, the prepared latex mixture was casted on a polytetrafluoroethylene (PTFE) plate and then dried at 50 °C for 3 hours to form the PS-Ag/P(St-BA) L-anisotropic conductive films. The content of PS-Ag particles in the PS-Ag/P(St-BA) L-anisotropic conductive film can be obtained from the following equation:

$$\text{Content of PS-Ag (wt.\%)} = \frac{W_{\text{PS-Ag}}}{W_{\text{PS-Ag}} + W_{\text{P(St-BA)}}} \times 100\%$$

where $W_{\text{PS-Ag}}$ and $W_{\text{P(St-BA)}}$ are dry weight.

Characterization

Properties of PS-Ag core-shell particles

Field emission scanning electron microscopy (FE-SEM, JEOL JSM-6330F) was used for the study of morphology and particle size distribution. The glass transition temperatures (T_g) of PS-SH and P(St-BA) particles were determined by a differential scanning calorimeter (DSC, TA Q20). Thermalgravimetric analyzer (TGA, TA Q50) was applied to test the thermal stability of the products and estimate the relative coating mass of Ag nanoparticles to the whole particles. Zeta-potential analyzer (Malvern Nano-ZS) was used to measure the interfacial potential of core-shell particles. Furthermore, the optical absorption spectrum of the conductive core-shell particles was detected by using a UV-visible spectrometer (Thermo Spectronic Helios γ) to correlate the variation of Ag nanoparticle size. Core-shell particles also were

characterized by means of a X-ray diffractometer (XRD, Rigaku Ultima IV) with monochromatic Cu K α radiation to reveal the crystallinity.

The electrical properties of PS-Ag core-shell particles were investigated by the following method. The PS-Ag latexes were dried in an air-circulating oven at 50°C for 1 day. Then, the dried powder of PS-Ag core-shell particles was compressed to form the tablets. The surface resistance was measured with a four point probe (Quatek QT-50) and the tablet thickness was measured by a micrometer (Mitutoyo 293-815). The conductivity of compressed tablets was evaluated by the following equation: $\sigma = 1/(DR)$, where R represents the surface resistance (Ω/\square), and D is the tablet thickness (cm).

Properties of PS-Ag/P(St-BA) large-scale anisotropic conductive films

The initial viscosities of PS-Ag/P(St-BA) latex mixtures were measured by a viscometer (Brookfield DV-E), and the shear rate remained at 1.4 (1/s). The surface resistance, thickness of conductive layer, and conductivity of PS-Ag/P(St-BA) L-anisotropic conductive films were investigated in this study. The top and bottom surface resistance were measured respectively by using a four point probe (Quatek QT-50) and the thickness of conductive layer could be obtained from the cross-section images of FE-SEM. The bottom layer conductivity of L-anisotropic conductive films was evaluated by the following equation: $\sigma = 1/(DR)$, where R represents the surface resistance (Ω/\square), D is the thickness of conductive layer (cm).

Bending and Stretching tests of the PS-Ag/P(St-BA) L-anisotropic conductive film were performed to detect the flexibility and stretchability via investigating the variation of surface resistance. The latex mixtures were coated on polytetrafluoroethylene plates to make the specimens. After drying, the L-anisotropic conductive films were cut into rectangular shape (1 cm x 2.5 cm) and used without additional treatment before the tests. In the bending test, every specimen was bent back and forth (180°) for 500 times (cycles). Stretching test was carried out via elongating the specimens to different ratios until broken. Moreover, the variation of surface resistance also was examined by stretching the specimens to 20% of strain for 1 second and releasing to the original length for 20-50 times.

Results and discussion

In the present study, monodispersed polystyrene particles were synthesized via emulsifier-free emulsion polymerization and the Ag nanoparticle layer was embedded onto the surface of polystyrene latex particles during the modified electroless plating process. Then, the core-shell particles were mixed with the soft P(St-BA) latex to make the L-anisotropic conductive films via gravity sedimentation method. The optoelectronic properties of the films with different contents of core-shell particles were measured and discussed.

Synthesis and characterization of monodispersed polystyrene-silver core-shell particles

The experimental procedure was summarized in **Scheme 1**. At first, the polymerization was terminated when the PS particles had achieved a conversion of

60-70%, the obtained particles were used as the polymeric cores in the second stage. Due to the solubility of polymers to monomers and the reactivity of Si-OH groups, the monodispersed PS nanospheres with mercaptan groups were synthesized successfully. The morphology of PS colloids prepared by emulsifier-free emulsion polymerization in the first and second stage was shown in **Figure 1**. As observed from the images, the size of PS particles grew from 320 nanometers to 480 nanometers after completing polymerization in the second stage. Moreover, as the content of TEVS increased, the PS colloids became more polydispersed due to the self-nucleation of SiOH-groups and its rapid reaction rate in the water phase. The DSC thermograms of PS with different swelling ratios of St, DVB, and TEVS were displayed in **Figure 2**. The T_g of PS_{4/3.5/2.5} was around 98 °C, and it would increase slightly as TEVS content in PS nanospheres was increasing. The result indicated that PS particles with a higher TEVS content would become more capable of crosslinking and had a wide range of particle size distribution as observed from **Figure 1**. Therefore, based on the above results, the PS_{4/2/6} particles were applied for the dielectric core throughout this study. The stability of dispersed PS nanospheres originated from the negative charge of KPS segments. In this modified electroless plating process as displayed in **Scheme 1**, the PS colloids without roughening by the sulfuric acid were sensitized directly through the adsorption of Sn²⁺ ions onto the surfaces via the chelation of the functional groups of mercaptan and the electrostatic interactions of positive-negative charges. The main purpose of sensitization was to increase the efficiency of Ag reduction and ensure the location of the reduced sites. After adding Ag(NH₃)₂⁺ solutions, Ag(NH₃)₂⁺ ions were attracted onto the surface of particles and then replaced the Sn²⁺ ions to form some Ag seeds via redox reaction. These metallic Ag seeds became the reducing center during the deposition of silver shells. Then, in order to guarantee the shell growth of silver

onto the PS particles, a weak reducing agent like glucose, which was common and environment friendly, was applied to reduce the $\text{Ag}(\text{NH}_3)_2^+$ complex ions to Ag nanoparticles. Ultimately, monodispersed polystyrene-silver core-shell composite particles could be obtained with compact Ag nanoshells.

Table 1 showed the value of zeta potential in each step during the overall process. At the beginning, the dissociation of KPS segments resulted in the negative charges for the polymerizing PS particles. The slight increase (less negative) in zeta potential observed from the PS nanospheres with the functional groups of mercaptan. Then, in the presence of Sn^{2+} ions on the PS surface, the value of zeta potential increased noticeably due to the offset of the negative charge. Interestingly, the value of zeta potential was decreased after the formation of the Ag nanoshells. This phenomenon was caused by the addition of sodium citrate tribasic dehydrate, and the complex ions would deposit onto the surface of Ag nanoparticles giving rise to the decrease of the surface potential.

The UV-vis absorption spectra during Ag reduction were represented in the **Figure 3**. All of the measured samples were diluted with DI water to the suitable concentration. Due to the collective oscillation of transporting electrons in answer to optical excitation, Ag nanoparticles represented the special properties of surface plasmon resonance (SPR).⁵⁰ At the beginning of Ag reduction, there was a characteristic peak around 401 nanometers observed. The absorption peak became red-shifted and broadening with the increasing of reducing time due to the growth of Ag nanoparticles.

Furthermore, in order to investigate the effect of sensitization, different experimental conditions were used. The results were shown in **Figure 4(a) and (b)**, and the SEM images showed that the Ag nanoparticles were much denser on the

PS-Ag core-shell particles with the addition of SnCl_2 . Apparently, due to the adsorption of Sn^{2+} ions onto the PS particles, the efficient redox reaction between Sn^{2+} ions and Ag^+ ions indeed enhanced the embedment of Ag nanoparticles on the surface. For the sake of improving the coverage significantly, PS-Ag core-shell particles with different content of Ag were also synthesized. The morphology, content of Ag, and electric properties were displayed in **Figure 4**, **Figure 5** and **Table 2**. With the increasing content of Ag, the nanoshells became thicker and denser which could be observed from the images. As the weight ratio of Ag increased from 50 wt.% to 90 wt.%, the average grain size of Ag nanoparticles deposited on the surface of PS particles increased from 20-30 nanometers to 120-140 nanometers, and the extent of surface coverage increased certainly. During the reduction process, the delayed addition of sodium citrate tribasic dehydrates would decrease the formation of complex, hence it resulted in decreasing the particle size of Ag nanoparticles and also improved the coverage of Ag nanoparticles as represented in **Figure 4(c) and (d)**. The content of Ag was examined by TGA and shown in **Figure 5**. The experimental values were almost the same as the feeding amounts of Ag, and the results proved that all of the Ag were reduced successfully during the period of redox reaction. Moreover, the bulk electrical properties of PS-Ag core-shell particles were also measured to evaluate its potential for the electronic applications. As presented in the table, with the increasing content of Ag, the electric properties were raised remarkably. Meanwhile, the delayed addition of sodium citrate tribasic dehydrates also improved the conductivity noticeably owing to the denser packing of much smaller Ag nanoparticles. Interestingly, when the Ag content was up to 90 wt.%, equivalent to 46.4 vol.% of Ag existing in the core-shell particles, the conductivity was almost the same as that of the pure silver. **Figure 6** showed the XRD pattern of PS-Ag core-shell

particles. The strong diffraction peaks observed distinctly at 38.1, 44.4, 64.6, 77.5 and 81.4 (2θ degrees) were identified as the (1 1 1), (2 0 0), (2 2 0), (3 1 1) and (2 2 2) in the crystalline planes of the face-centered cubic Ag particles (JCPDS no. 04-0783), respectively. Sharp diffraction peaks indicated that a pure silver shell with high crystallinity was successfully synthesized on the PS surface. In summary, the above experimental results proved that the emulsifier-free emulsion polymerization provided the monodispersed cores steadily and the modified electroless silver plating process could ensure the dense embedment of Ag nanoparticles on the surface of PS nanospheres even though without the treatment of roughening.

Optoelectronic properties of PS-Ag/P(St-BA) large-scale anisotropic conductive film

In order to apply the PS-Ag core-shell particles with great optoelectronic properties to the flexible electronic devices, the PS-Ag core-shell particles and P(St-BA) latex ($T_g = -20\text{ }^\circ\text{C}$) were mixed and then coated on the polytetrafluoroethylene substrate.⁴⁸ After drying, a L-anisotropic conductive film would be obtained. In the following experiments, highly conductive PS_{4/2/6}-Sn-SC-Ag₉₀ core-shell particles were chosen as the filler in the L-anisotropic conductive films. The mechanism of L-anisotropic conductive film formation was proposed and depicted in **Scheme 2**. As the P(St-BA) latex was introduced into the PS-Ag core-shell conductive latex, the latex particles were well-distributed in the mixing period. The stability of this latex mixture stemmed from the negative charge repulsion. However, when the latex mixture was coated on the substrate and heated to dry, the PS-Ag conductive particles would subside to the bottom layer during the evaporation of water due to its high density. In addition, the mixed soft P(St-BA)

particles with low T_g started to fuse and became a continuous rubbery phase in the top layer and played an essential role in the connection of the PS-Ag core-shell conductive particles in the bottom layer. As a result, a L-anisotropic conductive network was constructed after the film-forming process.

At first, the prepared PS-Ag and P(St-BA) latexes were mixed at different ratios. The electrical properties of PS-Ag/P(St-BA) L-anisotropic conductive films were listed in **Table 3**, including top/bottom surface resistance, conductive layer thickness, and conductivity of the bottom surfaces. As the PS-Ag content was over 30 wt.% (corresponding to a Ag content of 4.54 vol.%), a substantially low surface resistance was obtained because of a sufficient connection of the conductive network. With the increasing content of PS-Ag, the surface resistances and its standard deviations reduced unceasingly due to the formation of the more uniform and continuous conductive network. When the content of PS-Ag was 50 wt.% (corresponding to a Ag content of 9.99 vol.%), the conductivity of the bottom surface in the L-anisotropic conductive film could reach 1.8×10^3 S/cm. However, as the PS-Ag content was above 60 wt.%, the L-anisotropic conductive films started to become brittle and fragmented, and the surface resistance was increasing suddenly. It indicated that the introduction of P(St-BA) latex indeed improved the connection among the core-shell conductive particles. Furthermore, in order to demonstrate the relationship between optimal percentage of fillers and conductive layer thickness, three samples with different conductive layer thicknesses were fabricated and the optimal results of surface resistance were shown in **Figure 7**. The optimal content of PS-Ag would move from 50 wt.% to 40 wt.% when the thickness of conductive layer varied from 100 μm to 380 μm . In other words, the optimal percentage of conductive fillers would decrease slightly as the thickness of conductive layer increased. **Figure 8** represented the

cross-sectional SEM images of PS-Ag/P(St-BA) L-anisotropic conductive films with different contents of PS_{4/2/6}-Sn-SC-Ag₉₀. As observed from the images, there was a distinct interface between the conductive and insulating layers from the content of 20 wt.% to 60 wt.% PS-Ag. However, when the amounts of filler increased above 70 wt.%, the interface between two layers disappeared owing to the reduction of the blending matrix. In other words, with the increase of fillers, the conductive network could not be preserved and lead to the increase of surface resistance. The results could be further interpreted as follows. In this study, PS-Ag/P(St-BA) latex mixture was casted on the PTFE substrate and dried in the air-circulating oven at 50°C for 3 hours to form the L-anisotropic conductive film. The settling of PS-Ag core-shell particles occurred during the evaporation of water, and the viscosity of latex mixture rose up successively upon drying. Herein, the initial viscosities of latex mixtures with different contents of PS_{4/2/6}-Sn-SC-Ag₉₀ were measured and depicted in **Figure 9**. As the content of PS-Ag was increased from 20 wt.% to 50 wt.%, the latex mixture stayed in low viscosity initially and the conductive PS-Ag core-shell particles could settle quickly to form a compact conductive layer. However, when the content of PS-Ag core-shell particles was above 70 wt.%, the viscosity of latex mixture rose up rapidly, so that the PS-Ag particles were not easy to pack as densely as the one with less fillers inside during the fabrication of L-anisotropic conductive films. That is to say, the conductive network was quite loose after drying, so the thickness of conductive layer became much bulky as shown in **Figure 8(d)**, which led to the increase of surface resistance. Furthermore, it is worth noting that a percolation threshold was observed around 70 wt.% of PS-Ag for the surface resistance of the top surface due to the reduced amounts of insulation matrix, which brought about the electron transportation in the overall conductive film.

Based on these results, 30 wt.% to 60 wt.% of fillers in the PS-Ag/P(St-BA) L-anisotropic conductive films were chosen to test their flexibility and stretchability, and the surface resistance was measured in the central part of L-anisotropic conductive films as displayed in **Scheme 3**. In our previous work, a great enhancement of flexibility was received from the introduction of the soft matrix.⁴³⁻⁴⁴ The bending test results for determining the flexibility of L-anisotropic conductive films were measured. In order to avoid the affection of original surface resistance on the result of the bending test, the surface resistance ratio (R/R_0) was utilized, where R and R_0 meant the surface resistance after and before bending, respectively. The surface resistance of PS-Ag/P(St-BA) L-anisotropic conductive films only increased a slight value ($R/R_0 < 1.6$) after 500 bending cycles when the content of PS-Ag conductive particle was from 30 wt.% to 60 wt.%. It indicated that the introduction of P(St-BA) latex could improve the flexibility of L-anisotropic conductive films validly.

Furthermore, **Figure 10(a)** and **Figure 11** showed the results of the stretching tests of PS-Ag/P(St-BA) L-anisotropic conductive films with respect to different contents of fillers. At the beginning, the L-anisotropic conductive films were stretched to its maximum length to test its elongation capability. As the PS-Ag content was 30 wt.%, the L-anisotropic conductive films could be stretched to 60% and the surface resistance only increased 3.41 times compared to the original value. In other words, the stretchable L-anisotropic conductive films still could preserve the conductive network effectively. With increasing PS-Ag content, the L-anisotropic conductive films became easier to fracture owing to the reduction of soft polymeric matrix. When the PS-Ag content was above 60 wt.%, the surface resistance was increased significantly. Hence, a sufficient amount of soft latex, P(St-BA), was needed to remain good stretchability. Moreover, the variation of surface resistance of film under

cycles of stretching tests was also investigated and shown in **Figure 10(b)**. When the PS-Ag content was 30 wt.%, the L-anisotropic conductive films could be stretched to 20 % for 50 times and the surface resistance only increased 2.89 times compared to the original value. Owing to the decrease of P(St-BA) matrix, the L-anisotropic conductive films became easier to break and could not recover to the original length. Therefore, as the PS-Ag content was 50 wt.%, the surface resistance increased 10.98 times for stretching 30 times, and if the PS-Ag content was 60 wt.%, the surface resistance would increase 22.74 times for only 20 times. The above results proved that the introduction of soft matrix indeed could enhance the flexibility and stretchability efficiently.

Conclusions

Novel large-scale anisotropic conductive films had been produced by a facile gravity sedimentation method. Monodispersed core-shell particles with PS as core and the Ag nanoparticles as shell had been successfully synthesized by emulsifier-free emulsion polymerization. Many parameters were considered and selected to improve the conductivity and coverage of Ag nanoparticles on the PS sphere surface. The obtained particles with diameters about 600 nanometers were observed from the SEM images. As the Ag content was increased, the conductivity of the PS-Ag core-shell particles was enhanced to a great extent with the addition of SnCl_2 and sodium citrate tribasic dehydrate in the electroless plating process. Furthermore, the high conductive PS-Ag core-shell particles could be mixed with soft latex P(St-BA) to form the L-anisotropic conductive films successfully via the gravity sedimentation. The L-anisotropic conductive films made of the PS-Ag core-shell particles exhibited good conductivity on the bottom surface while insulation on the top surface. Most

importantly, the flexibility of the L-anisotropic conductive films was raised significantly. After 500 bending cycles, the increase in surface resistance was only less than 1.6 times of its original value at the content of 30 wt.% to 60 wt.% PS-Ag conductive particles. Furthermore, during the stretching tests, the L-anisotropic conductive film could be stretched to 60% and the surface resistance increased only 3.41 times of its original value at the content of 30 wt.% PS-Ag conductive particles. It could be stretched to 20% for 50 times and the surface resistance only increased 2.89 times. It indicated that the L-anisotropic conductive films were flexible and stretchable, and the conductive network could be preserved upon bending and stretching. The present study suggests that the addition of P(St-BA) matrix effectively improves the film flexibility and stretchability, and it has potential applications for high performance anisotropic conductive films in the electronic industries.

Acknowledgements

The financial supports from the National Science Council of Taiwan and Industrial Technology Research Institute are highly appreciated.

Figure Captions

Scheme 1. The preparation route of PS-Ag core-shell particles.

Scheme 2. The formation of L-anisotropic conductive film using PS-Ag core-shell particles as fillers.

Scheme 3. Bending and stretching tests on the L-anisotropic conductive film.

Figure 1. The SEM images of PS particles prepared from emulsifier-free emulsion polymerization (a) PS with the conversion about 60-70% in the first stage (b) PS_{4/3.5/2.5}, (c) PS_{4/2/6}, (d) PS_{4/2/10}.

Figure 2. The DSC curves of PS-SH particles prepared from emulsifier-free emulsion polymerization.

Figure 3. The UV-vis absorption spectra of PS-Ag core-shell particles during Ag reduction.

Figure 4. The morphology of PS-Ag core-shell particles (a) PS_{4/2/6}-Ag₅₀, (b) PS_{4/2/6}-Sn-Ag₅₀, (c) PS_{4/2/6}-Sn-Ag₈₀, (d) PS_{4/2/6}-Sn-SC-Ag₈₀, (e) PS_{4/2/6}-Sn-SC-Ag₉₀.

Figure 5. The TGA curves of PS-Ag core-shell particles.

Figure 6. The XRD pattern of PS_{4/2/6}-Sn-SC-Ag₉₀ core-shell particle.

Figure 7. The film surface resistance of PS-Ag/P(St-BA) L-anisotropic conductive films with different PS_{4/2/6}-Sn-SC-Ag₉₀ contents. Three samples with different conductive layer thickness were fabricated, (a) 100 μm (b) 260 μm (c) 380 μm.

Figure 8. The cross-section SEM images of PS-Ag/P(St-BA) L-anisotropic conductive films with different contents of PS_{4/2/6}-Sn-SC-Ag₉₀ (a) 20 wt.%, (b) 30 wt.%, (c) 50 wt.%, (d) 80 wt.%.

Figure 9. The initial viscosity of PS-Ag/P(St-BA) latex mixtures with different contents of PS_{4/2/6}-Sn-SC-Ag₉₀. (shear rate= 1.4 1/s)

Figure 10. The relative surface resistance ratio (R/R₀) of the PS-Ag/P(St-BA)

L-anisotropic conductive films with different contents of PS_{4/2/6}-Sn-SC-Ag₉₀ for (a) stretching test, (b) stretching cycles.

Figure 11. The stretchable L-anisotropic conductive films during the stretching test (a) content of PS-Ag =30 wt.%, strain=0% (b) content of PS-Ag =30 wt.%, strain=60% (c) content of PS-Ag =60 wt.%, strain=0% (d) content of PS-Ag =60 wt.%, strain=60%.

Table lists

Table 1. the values of zeta potential in each step during the overall process

	PS particle ^a	PS-SH particle	PS-SH particle ^b	PS-Ag particle
Zeta potential (mV)	-64.7	-52.6	-19.1	-38.7

^a The conversion is about 60-70% in the first stage.

^b After the treatment of sensitization.

Table 2. The content of silver, surface resistance, compressed tablet thickness, and conductivity of PS-Ag particles.

Sample code	Ag weight percentage (wt.%) ^a	Ag volume percentage (vol.%) ^b	Resistance (Ω/\square)	Compressed tablet thickness (mm)	Bulk conductivity (S/cm)
PS _{4/2/6} -Ag ₅₀	49.1	8.9	0.0298	0.465	724
PS _{4/2/6} -Sn-SC-Ag ₅₀	49.3	9	0.0092	0.464	2340
PS _{4/2/6} -Sn-Ag ₈₀	77.1	25.5	0.0013	0.411	17700
PS _{4/2/6} -Sn-SC-Ag ₈₀	77.2	25.6	0.0003	0.405	82300
PS _{4/2/6} -Sn-SC-Ag ₉₀	89.5	46.4	0.0001	0.440	227000

^a The results were determined by TGA

^b The Ag volume percentages were calculated by the following equation:

$$\text{Volume percentage (vol\%)} = \frac{\frac{X_{\text{Ag}}}{\rho_{\text{Ag}}} + \frac{100 - X_{\text{Ag}}}{\rho_{\text{PS}}}}{X_{\text{Ag}} + \frac{100 - X_{\text{Ag}}}{\rho_{\text{PS}}}} \times 100\%, \text{ where } X_{\text{Ag}} \text{ meant the weight}$$

percentage of Ag, ρ_{Ag} (10.49 g/cm³)⁵¹ and ρ_{PS} (1.05 g/cm³)⁵² represent the density of Ag and PS, respectively.

Table 3. The film surface resistance, conductive layer thickness, and conductivity of PS-Ag /P(St-BA) L-anisotropic conductive films with different PS_{4/2/6}-Sn-SC-Ag₉₀ contents.

PS _{4/2/6} -Sn-SC-Ag ₉₀ (wt.%)	bottom surface resistance(Ω/\square)	Top surface resistance(Ω/\square)	Conductive layer thickness (μm)	Conductivity of bottom surface (S/cm) ^a
20	0.1641±0.0423	>200M	260	248±67.98
30	0.0495±0.0199	>200M	260	886±362.48
40	0.0220±0.0049	>200M	260	1826±459.38
50	0.0215±0.0038	>200M	260	1827±320.21
60	0.0564±0.0086	>200M	260	696±119.97
70	0.1502±0.0281	38±7.07	315	216±38.14
80	0.1732±0.0308	0.1467±0.0171	320	184±30.92

^a The conductivity of conductive layer.

Notes and references

^a Department of Chemical Engineering, National Taiwan University, Taipei, Taiwan. E-mail: chenwc@ntu.edu.tw, ycchiu@ntu.edu.tw; Fax: +886-2-23623259; Tel: +886-2-23623259

^b Institute of Polymer Science and Engineering, National Taiwan University, Taipei, Taiwan

^c Department of Chemical Engineering & Biotechnology, National Taipei University of Technology, Taipei, Taiwan.

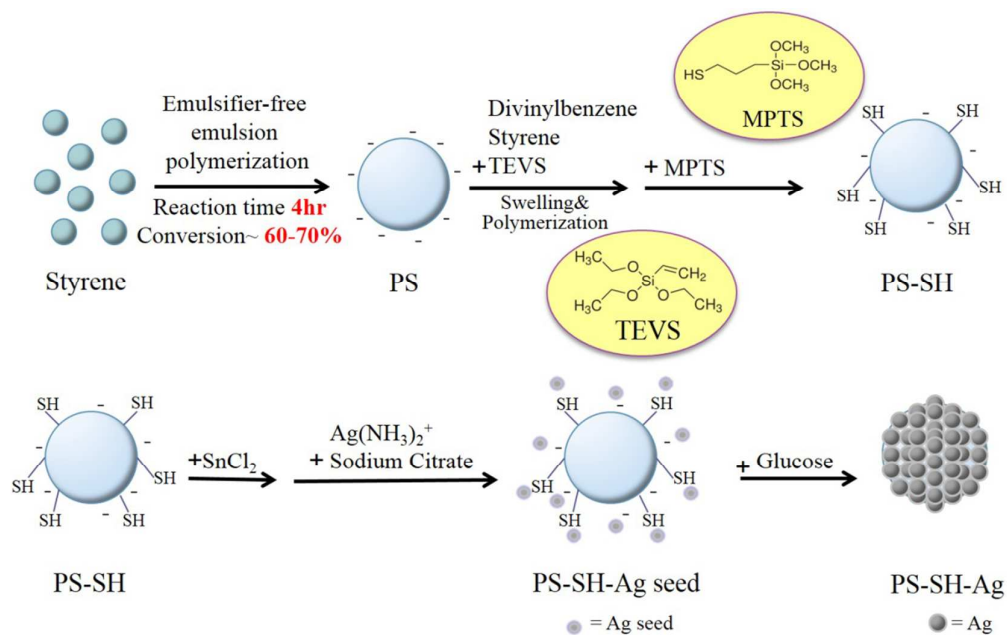
^d Department of Cosmetic Science and Institute of Cosmetic Science, Chia Nan University of Pharmacy and Science, Tainan, Taiwan.

^e Department of Material Science and Engineering, National Taiwan University, Taipei, Taiwan

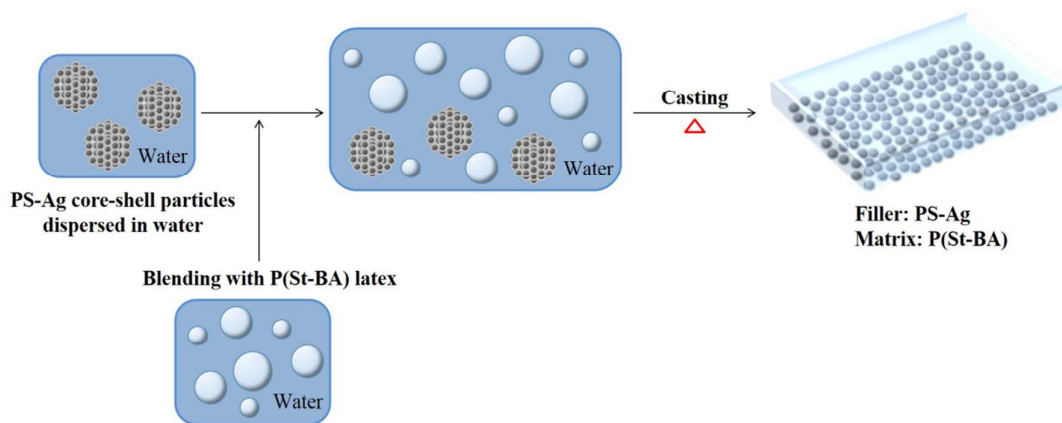
- 1 Z. Deng, M. Chen, L. Wu, *J. Phys. Chem. C*, 2007, **111**, 11692.
- 2 S. Tokonami, Y. Yamamoto, Y. Mizutani, I. Ota, H. Shiigi, T. Nagaoka, *J. Electrochem. Soc.*, 2009, **156**, 558.
- 3 J. Zhang, J. Liu, S. Wang, P. Zhan, Z. Wang, N. Ming, *Adv. Funct. Mater.*, 2004, **14**, 1089.
- 4 J.-H. Lee, M.A. Mahmoud, V.B. Sitterle, J.J. Sitterle, J.C. Meredith, *Chem. Mater.*, 2009, **21**, 5654.
- 5 M. Agrawal, S. Gupta, M. Stamm, *J. Mater. Chem.*, 2011, **21**, 615.
- 6 F. Caruso, *Adv. Mater.*, 2001, **13**, 11.
- 7 E. Bourgeat-Lami, *J. Nanosci. Nanotechnol.*, 2002, **2**, 1.
- 8 P.D. Cozzoli, T. Pellegrino, L. Manna, *Chem. Soc. Rev.*, 2006, **35**, 1195.
- 9 Q. Zhang, J. Ge, J. Goebel, Y. Hu, Y. Sun, Y. Yin, *Adv. Mater.*, 2010, **22**, 1905.
- 10 W. Zhao, Q. Zhang, H. Zhang, J. Zhang, *J. Alloy. Compd.*, 2009, **473**, 206.
- 11 S.-M. Chang, J.-H. Jou, A. Hsieh, T.-H. Chen, C.-Y. Chang, Y.-H. Wang, C.-M. Huang, *Microelectron. Reliabi.*, 2001, **41**, 2001.
- 12 M.-J. Yim, K.-W. Paik, *Proceedings., The First IEEE International Symposium on.*

- IEEE*, 1997, 233.
- 13 V. G. Pol, D. N. Srivastava, O. Palchik, V. Palchik, M. A. Slifkin, A. M. Weiss, A. Gedanken, *Langmuir*, 2012, **18**, 3352.
 - 14 V. G. Pol, A. Gedanken, J. Calderon-Moreno, *Chem. Mater.*, 2003, **15**, 1111.
 - 15 V. Prasad, A. Mikhailovsky, J. A. Zasadzinski, *Langmuir*, 2005, **21**, 7528.
 - 16 V. G. Pol, H. Grisaru, A. Gedanken, *Langmuir*, 2005, **21**, 3635.
 - 17 C. W. Chen, T. Serizawa, M. Akashi, *Langmuir*, 1999, **15**, 7998.
 - 18 C. Tian, E. Wang, Z. Kang, B. Mao, C. Zhang, Y. Lan, C. Wang, Y. Song, *J. Solid State Chem.*, 2006, **179**, 3270.
 - 19 J.-H. Lee, D. O. Kim, G.-S. Song, Y. Lee, S.-B. Jung, J.-D. Nam, *Macromol. Rapid Comm.*, 2007, **28**, 634.
 - 20 Y. Lu, Y. Mei, M. Schrunner, M. Ballauf, M. W. Möller, J. Breu, *J. Phys. Chem. C*, 2007, **111**, 7676.
 - 21 I. Yamaguchi, M. Watanabe, T. Shinagawa, M. Chigane, M. Inaba, A. Tasaka, M. Izaki, *ACS Appl. Mater. Inter.*, 2009, **1**, 1070.
 - 22 A. G. Dong, Y. J. Wang, Y. Tang, N. Ren, W. L. Yang, Z. Gao, *Chem. Commun.*, 2002, 350.
 - 23 T. Ji, V. G. Lirtsman, Y. Avny, D. Davidov, *Adv. Mater.*, 2001, **13**, 1253.
 - 24 Z. Liang, A. Susha, F. Caruso, *Chem. Mater.*, 2003, **15**, 3176.
 - 25 C. Song, D. Wang, Y. Lin, Z. Hu, G. Gu, X. Fu, *Nanotechnology*, 2004, **15**, 962.
 - 26 K. Kim, H. B. Lee, H. K. Park, K. S. Shin, *J. Colloid Interface Sci.*, 2008, **318**, 195.
 - 27 Y.-C. Chen, R. L.-H. Liu, X.-L. Chen, H.-J. Shu, and M.-D. Ger, *Appl. Surf. Sci.*, 2011, **257**, 6734.
 - 28 Y. Kobayashi, V. Salgueirino-Maceira, L. M. Liz-Marzán, *Chem. Mater.*, 2001, **13**, 1630.
 - 29 Z. Chen, Z. L. Wang, P. Zhan, J. H. Zhang, W. Y. Zhang, H. T. Wang, N. B. Ming, *Langmuir*, 2004, **20**, 3042.
 - 30 K.-J. Lin, H.-M. Wu, Y.-H. Yu, C.-Y. Ho, M.-H. Wei, F.-H. Lu, W. J. Tseng, *Appl. Surf. Sci.*, 2013, **282**, 741.
 - 31 Y. Ma, Q. Zhang, Y. Li, *J. Electrochem. Soc.*, 2011, **159**, 119.
 - 32 Y. Ma, Q. Zhang, *Appl. Surf. Sci.*, 2012, **258**, 7774.
 - 33 W. Zhao, Q. Zhang, J. Zhang, H. Zhang, *Polym. Composites*, 2009, **30**, 891.
 - 34 J. A. Rogers, T. Someya, Y. Huang, *Science*, 2010, **327**, 1603.
 - 35 R. F. Service, *Science*, 2003, **301**, 909.
 - 36 B. Y. Ahn, E. B. Duoss, M. J. Motala, X. Guo, S.-I. Park, Y. Xiong, J. Yoon, R. G. Nuzzo, J. A. Rogers, J. A. Lewis, *Science*, 2009, **323**, 1590.
 - 37 T. Sekitani, Y. Nouguchi, K. Hata, T. Fukushima, T. Aida, T. Someya, *Science*, 2008, **321**, 1468.
 - 38 K. Takei, T. Takahashi, J. C. Ho, H. Ko, A. G. Gillies, P. W. Leu, R. S. Fearing, A. Javey, *Nat. Mater.*, 2010, **9**, 821.
 - 39 D. J. Lipomi, J. A. Lee, M. Vosgueritchian, B. C. K. Tee, J. A. Bolander, Z. Bao, *Chem. Mater.*, 2012, **24**, 373.
 - 40 P. Lee, J. Lee, H. Lee, J. Yeo, S. Hong, K. H. Nam, D. Lee, S. S. Lee, S. H. Ko, *Adv. Mater.*, 2012, **24**, 3326.
 - 41 D. J. Lipomi, Z. Bao, *Energy Environ. Sci.*, 2011, **4**, 3314.
 - 42 D. J. Lipomi, M. Vosgueritchian, B. C.-K. Tee, S. L. Hellstrom, J. A. Lee, C. H. Fox, Z. Bao, *Nat. nanotechnol.*, 2011, **6**, 788.
 - 43 *US pat.*, 5 604 379, 1997.
 - 44 *US pat.*, 5 918 113, 1999.
 - 45 R. S. Pai, K. M. Walsh, *J. Micromech. Microeng.*, 2005, **15**, 1131.

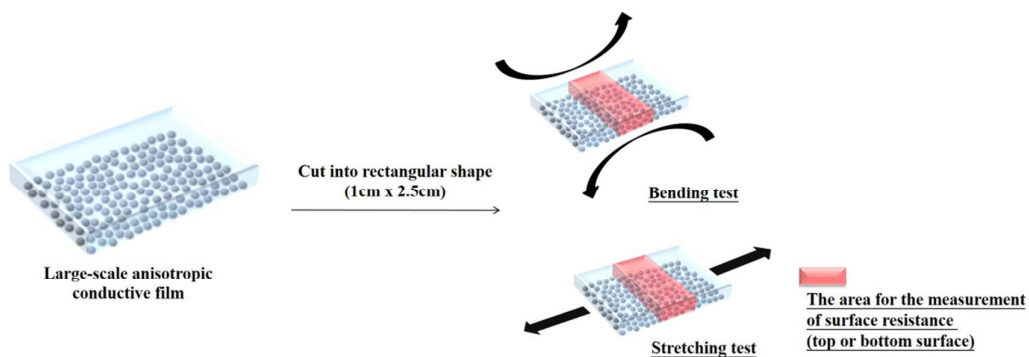
- 46 K. -S. Kim, C. -W. Ha, T. -Y. Jang, S. W. Joung, W. -S. Yun, *J. Micromech. Microeng.*, 2010, **20**, 105015.
- 47 H. -V. Nguyen, T. Eggen, B. Sten-Nilsen, K. Imenes, K. E. Aasmundtveit, *Electronic Components and Technology Conference*, Orlando, 2014.
- 48 H.-E. Yin, C.-H. Wu, K.-S. Kuo, W.-Y. Chiu, H.-J. Tai, *J. Mater. Chem.*, 2012, **22**, 3800.
- 49 H.-Y. Chen, H.-P. Shen, C.-H. Wu, W.-Y. Chiu, W.-C. Chen, H.-J. Tai, *J. Mater. Chem. C*, 2013, **1**, 5351.
- 50 K. T. Yong, Y. Sahoo, M. T. Swihart, P. N. Prasad, *Colloid Surface A*, 2006, **290**, 89.
- 51 S. Y. Yeo, S. H. Jeong, *Polym. Int.*, 2003, **52**, 1053.
- 52 A. Russom, A. K. Gupta, S. Nagrath, D. Di Carlo, J. F. Edd, M. Toner, *New J. Phys.*, 2009, **11**, 075025.



Scheme 1. The preparation route of PS-Ag core-shell particles.



Scheme 2. The formation of L-anisotropic conductive film using PS-Ag core-shell particles as fillers.



Scheme 3. Bending and stretching tests on the L-anisotropic conductive film.

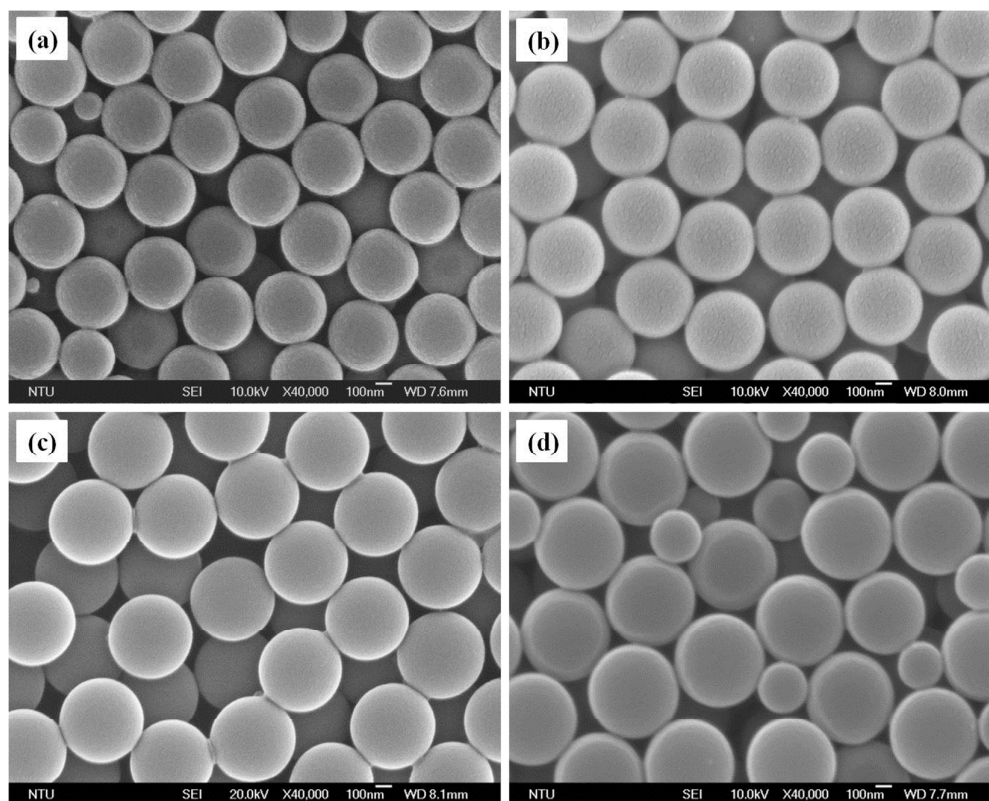


Figure 1. The SEM images of PS particles prepared from emulsifier-free emulsion polymerization (a)PS with the conversion about 60-70% in the first stage (b) $PS_{4/3.5/2.5}$, (c) $PS_{4/2/6}$, (d) $PS_{4/2/10}$.

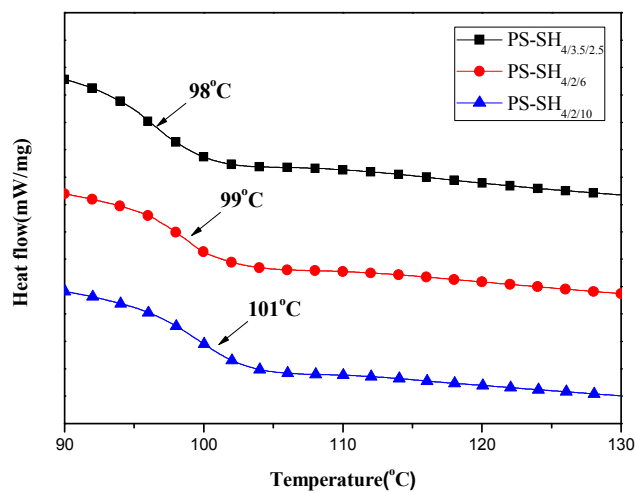


Figure 2. The DSC curves of PS-SH particles prepared from emulsifier-free emulsion polymerization.

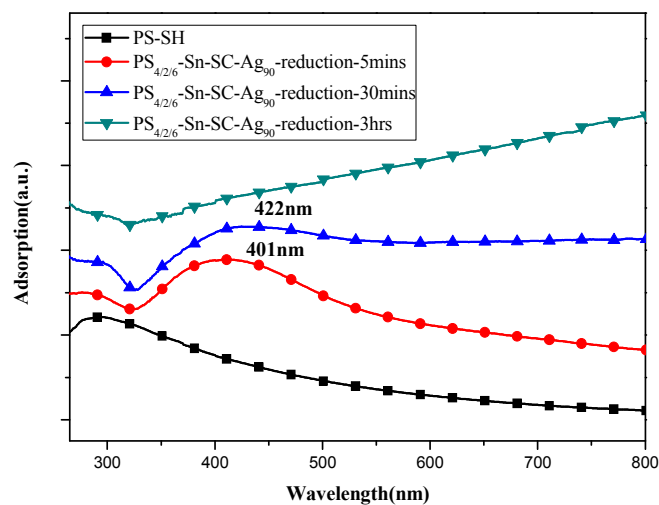


Figure 3. The UV-vis absorption spectra of PS-Ag core-shell particles during Ag reduction.

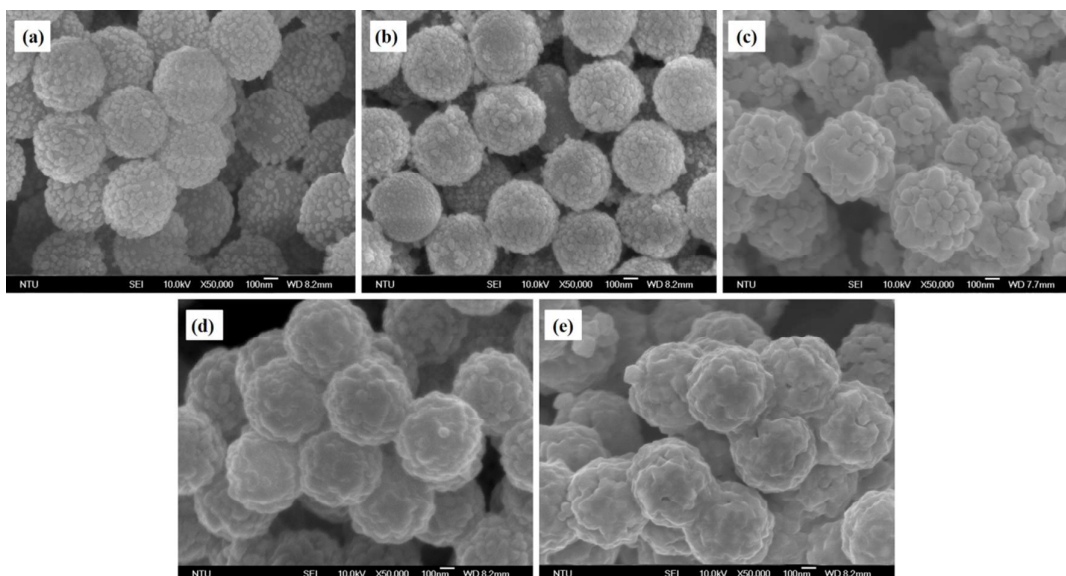


Figure 4. The morphology of PS-Ag core-shell particles (a) $\text{PS}_{4/2/6}\text{-Ag}_{50}$, (b) $\text{PS}_{4/2/6}\text{-Sn-Ag}_{50}$, (c) $\text{PS}_{4/2/6}\text{-Sn-Ag}_{80}$, (d) $\text{PS}_{4/2/6}\text{-Sn-SC-Ag}_{80}$, (e) $\text{PS}_{4/2/6}\text{-Sn-SC-Ag}_{90}$.

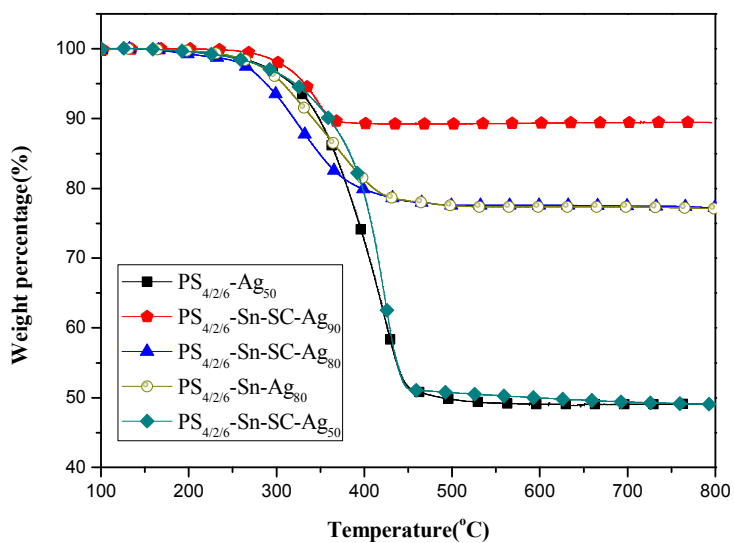


Figure 5. The TGA curves of PS-Ag core-shell particles.

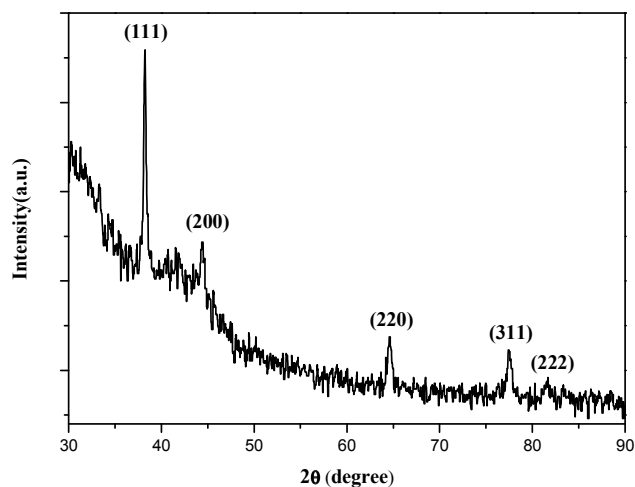


Figure 6. The XRD pattern of $\text{PS}_{4/2/6}\text{-Sn-SC-Ag}_{90}$ core-shell particles.

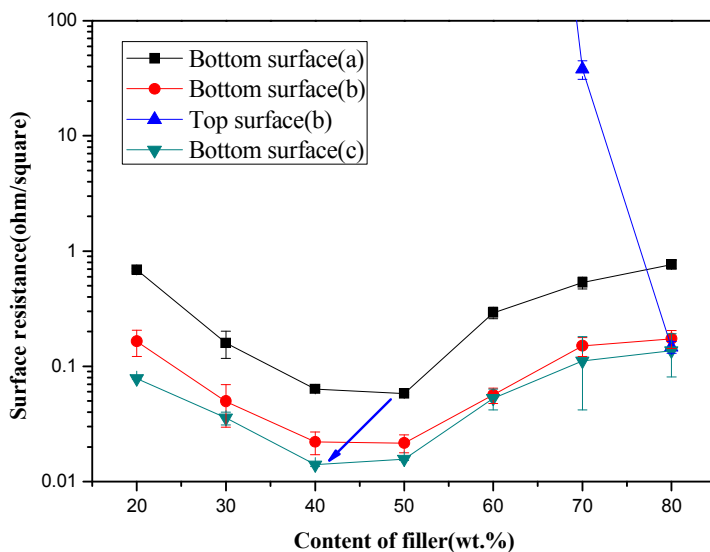


Figure 7. The film surface resistance of PS-Ag/P(St-BA) L-anisotropic conductive films with different $\text{PS}_{4/2/6}\text{-Sn-SC-Ag}_{90}$ contents. Three samples with different conductive layer thickness were fabricated, (a) $100 \mu\text{m}$ (b) $260 \mu\text{m}$ (c) $380 \mu\text{m}$.

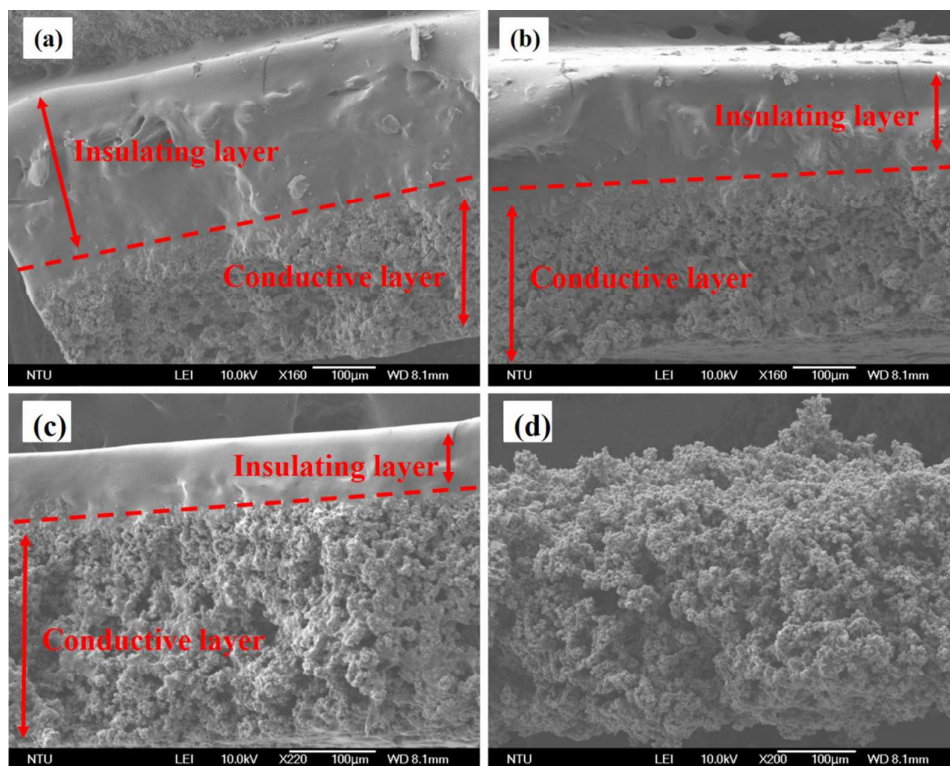


Figure 8. The cross-section SEM images of PS-Ag/P(St-BA) L-anisotropic conductive films with different contents of PS_{4/2/6}-Sn-SC-Ag₉₀ (a)20 wt.%, (b)30wt.%, (c)50wt.%, (d)80wt.%.

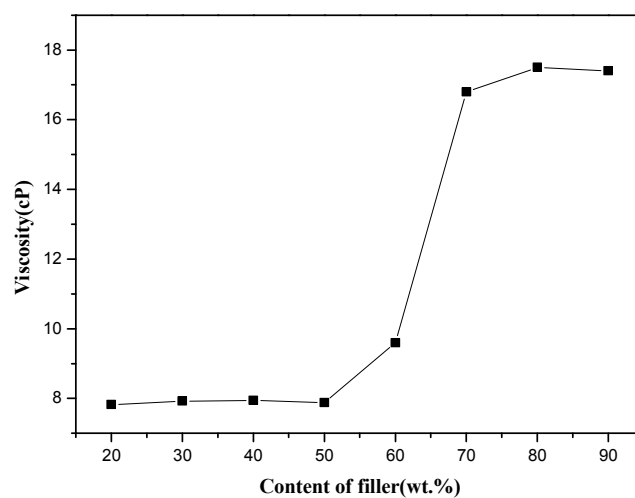


Figure 9. The initial viscosity of PS-Ag/P(St-BA) latex mixtures with different contents of PS_{4/2/6}-Sn-SC-Ag₉₀. (shear rate= 1.4 1/s)

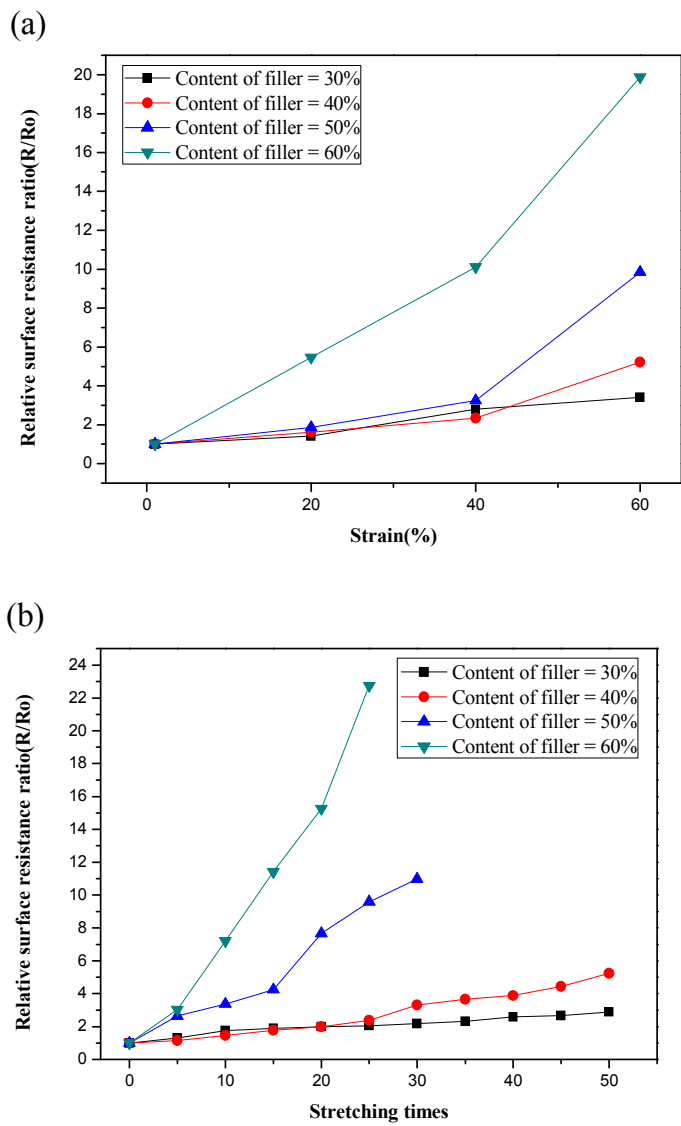


Figure 10. The relative surface resistance ratio(R/R_0) of the PS-Ag/P(St-BA) L-anisotropic conductive films with different contents of $PS_{4/2/6}$ -Sn-SC-Ag₉₀ for (a) stretching test, (b) stretching cycles (strain=20%).

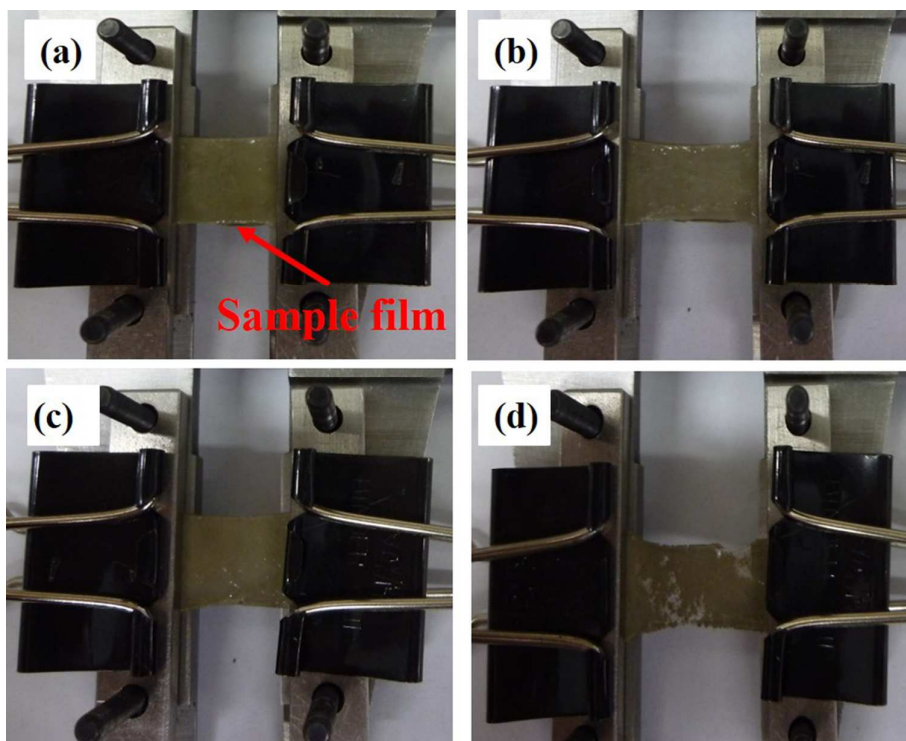


Figure 11. The stretchable L-anisotropic conductive films during the stretching test (a) content of PS-Ag =30 wt.%, strain=0% (b) content of PS-Ag =30 wt.%, strain=60% (c) content of PS-Ag =60 wt.%, strain=0% (d) content of PS-Ag =60 wt.%, strain=60%.

Graphical abstract

Keywords: polystyrene-silver core-shell particles, soft latex, poly(styrene-co-butyl acrylate) particles, gravity sedimentation, anisotropic conductive film.

Synthesis of Monodispersed Polystyrene-Silver Core-Shell Particles and Their Application for Fabrication of Stretchable Large-Scale Anisotropic Conductive Films

By Hsueh-Yung Chen,^a Hsiu-Ping Shen,^b Hung-Chin Wu,^a Man-Sheng Wang,^c Chia-Fen Lee,^d Wen-Yen Chiu,^{*abc} Wen-Chang Chen,^{*a}

An innovative and facile method is proposed to prepare the large-scale anisotropic conductive films incorporating with the organic/inorganic core-shell conductive particles.

